

Dracocephalum palmatum Stephan extract induces caspase- and mitochondria-dependent apoptosis via Myc inhibition in diffuse large B cell lymphoma

JISU KIM^{1,2}, JEONG NAM KIM³, INMYOUNG PARK⁴, SARDANA SIVTSEVA⁵,
ZHANNA OKHLOPKOVA⁵, ISMAYIL S. ZULFUGAROV^{5,6} and SANG-WOO KIM²

Departments of ¹Integrated Biological Science, ²Biological Sciences and ³Microbiology, Pusan National University, Busan 46241; ⁴Department of Asian Food and Culinary Arts, Youngsan University, Busan 48015, Republic of Korea; ⁵Department of Biology, North-Eastern Federal University, Yakutsk 677027, Russia; ⁶Institute of Molecular Biology and Biotechnology, Azerbaijan National Academy of Sciences, Baku, AZ 1073, Azerbaijan

Received November 12, 2019; Accepted June 25, 2020

DOI: 10.3892/or.2020.7797

Abstract. *Dracocephalum palmatum* Stephan (DPS), a medicinal plant used by Russian nomads, has been known to exhibit antioxidant properties. However, to the best of our knowledge, its anticancer effect has not been elucidated. The present study aimed to evaluate the tumor-suppressive effect of DPS extract (DPSE) in diffuse large B cell lymphoma (DLBCL) and the underlying mechanism. MTS assays and Annexin V staining were performed to assess the anti-proliferative and apoptotic effects of DPSE, respectively. To reveal the underlying mechanisms, the levels of pro- and anti-apoptotic Bcl-2 members were analyzed by western blotting. Rescue experiments were performed to investigate the potential involvement of Myc in DPSE-induced tumor-inhibitory effects. Additionally, high-performance liquid chromatography analysis was performed to analyze the components with anticancer effects. Exposure of multiple DLBCL cell lines to DPSE significantly decreased cell viability and increased apoptosis, whereas it had no effect on the survival of normal cells *in vitro* and *in vivo*. This indicates that its cytotoxic effect may be specific to cancer cells. Mechanistically, cell death induced by DPSE was dependent on the activation of caspase-3/7 and the disruption of mitochondrial membrane potential. Treatment with the extract ameliorated the expression of anti-apoptotic Bcl-2 members

Bcl-xL and Mcl-1, and upregulated that of pro-apoptotic Bcl-2 members Bax and Bak. These modulations led to the disruption of mitochondrial membrane potential, which culminated in the activation of executioner caspases-3 and -7. Notably, overexpression of Myc inhibited DPSE-induced cell killing, indicating the involvement of Myc in this process. Given that dysregulation of Myc is strongly associated with the pathobiology of DLBCL, the present study highlights the potential therapeutic efficacy of DPSE in patients with DLBCL with aberrant Myc expression. Furthermore, fractionation of DPSE by thin layer chromatography and liquid chromatography/mass spectrometry-based investigation of the fraction with bioactive compounds demonstrated that flavonoids may be responsible for most, if not all, of the anti-lymphoma effect. Efforts to identify the bioactive flavonoids is currently underway.

Introduction

Diffuse large B cell lymphoma (DLBCL) is the most frequent subtype of non-Hodgkin lymphoma (1). This blood cancer is further divided into germinal center B cell-like (GCB) and activated B cell-like (ABC) DLBCL according to gene expression profiling. Genetic lesions that characterize GCB DLBCL include deletion of phosphatase and tensin homolog and p53 mutations that are associated with genomic instability (2,3). Constitutively active NF- κ B signaling is the most prominent feature of the ABC subtype (1-3). The cyclophosphamide, doxorubicin, vincristine and prednisone regimen is established as the standard treatment of patients with DLBCL, and the addition of rituximab significantly improves overall survival without a significant increase in toxicity (4,5). However, 30-40% of patients with DLBCL still succumb to the disease worldwide, demanding a better understanding of the disease and continued efforts for drug development (6).

Apoptosis, or programmed cell death, is a tightly regulated process that is generally characterized by cell shrinkage, genomic DNA fragmentation, karyorrhexis and blebbing (7). The extrinsic apoptosis pathway occurs when extracellular death ligands, such as Fas-L or TNF- α , bind to

Correspondence to: Professor Sang-Woo Kim, Department of Biological Sciences, Pusan National University, 2 Busandaehak-ro 63beon-gil, Geumjeong, Busan 46241, Republic of Korea
E-mail: kimsw@pusan.ac.kr

Professor Ismayil S. Zulfugarov, Department of Biology, North-Eastern Federal University, 58 Belinsky Street, Yakutsk 677027, Russia
E-mail: iszulfugarov@yahoo.com

Key words: *Dracocephalum palmatum* Stephan, diffuse large B cell lymphoma, Myc, apoptosis, cell survival

their cognate death receptors, forming the death-inducing signaling complex (DISC) (7-9). DISC regulates the activation of pro- and anti-apoptotic Bcl-2 family members, which results in a decrease in the mitochondrial membrane potential, cytochrome *c* release, and activation of caspases-3 and -7. The intrinsic apoptosis pathway is initiated by endoplasmic reticulum stress, DNA damage, hypoxia or metabolic stress, and involves the disruption of mitochondrial outer membrane permeabilization and activation of caspases (10,11).

Dracocephalum palmatum Stephan (DPS), a medicinal plant used by Russian nomads, has been shown to exhibit strong antioxidant properties owing to high concentrations of phenolic compounds (12). However, to the best of our knowledge, its anti-lymphoma effect has not been characterized. The current study investigated the growth-suppressive and pro-apoptotic effect of DPS extract (DPSE) on DLBCL cells. Furthermore, thin layer chromatography (TLC) fractionation, followed by liquid chromatography/mass spectrometry-based analysis of the fraction with bioactive compounds, revealed that the anti-lymphoma effect of DPSE mainly stems from flavonoids.

Materials and methods

Preparation of DPSE. The well-dried DPS herbs were ground using a pestle and mortar until it was in a fine powder condition. After adding 100 ml 70% ethanol to 2 g fine powder, the mixture was shaken for 72 h on a rotary shaker to extract the majority of the compounds. The resulting extract was filtrated twice through a filter paper. The filtrated extract was concentrated and dried on an IKA RV10 BasicV rotary evaporator (IKA® Korea. Ltd.), and the dried extract was dissolved in an ultrasonic bath with the gradual addition of a total of 7 ml pure methanol. The resulting extract was stored in a freezer at -30°C.

Fractionation of the methanolic DPSE. Compound fractions were separated by TLC with the solvent system ethyl acetate, formic acid, glacial acetic acid and distilled water in a ratio of 100:11:11:26 (v/v), and with rutin (0.05% in methanol) as a standard. DPSE (600 μ l) was added to the TLC Sorbfil plates (20 μ l per 1 cm extract and 3 μ l per point standards; Sorbfil). Following separation, the TLC plates were examined and under ultraviolet (UV) light using the TLC-scanner. The developed spots were described by color and the R_f values are calculated based of the rutin standard with a R_f of 0.30. Under UV light, six fluorescent dark violet spots were detected with R_f values of 0.37, 0.50, 0.65, 0.75 and 0.90, which were designated as 1F, 2F, 3F, 4F, 5F and 6F, respectively. The developed spots were cut from the TLC plate in strips, crushed and placed into 15 ml Falcon tubes for elution in small volumes of pure 100% methanol in a Multi RS-60 Biosan multitorator (Biosan) for 20 min. The eluates were transferred to 10 ml tubes and centrifuged at 3,500 x g for 15 min at room temperature and freeze-dried. All chemicals used were chromatography grade purity.

High-performance liquid chromatography (HPLC) analysis. To analyze the components of the TLC fraction 6F of DPSE, the HPLC system (Agilent Technologies 1290 Series; Agilent Technologies, Inc.) was used. HPLC analysis was

performed using a Poroshell column (100x3.0 mm, 2.7 μ m). Mobile phase A was 0.1% formic acid in distilled water and mobile phase B was 0.1% formic acid in acetonitrile. The injection volume was 3 μ l, the column temperature was 40°C, and the samples were eluted at 300 μ l/min with gradient program (0-5 min, 2% B; 5-16 min, 40% B; 16-24 min, 95% B; 24-25 min, 2% B). The eluents separated from 6F were analyzed with Agilent Technologies 6530 Accurate-Mass (Q-TOF) (Agilent Technologies, Inc.). The optimal parameters were as follows: The positive ESI mode, gas temperature 300°C, sheath gas temperature 350°C, sheath gas flow rate 11 l/min, and fragmentor voltage 175 V.

Cell culture, reagents and antibodies. Human DLBCL cell lines (DHL4, DHL6, Ly1, Ly8, Ly19 and HBL1) (13) and peripheral blood mononuclear cells (PBMCs) were maintained in RPMI-1640 medium (Hyclone; Cytiva) supplemented with 10% fetal bovine serum (FBS; Hyclone; Cytiva), 1% L-glutamine, 1% N-2-hydroxyethylpiperazine-N'-2-ethanesulfonic acid buffer, and 1% penicillin/streptomycin at 37°C in a 5% CO₂ incubator. The DHL4, DHL6, Ly1, Ly8, Ly19 and HBL1 DLBCL cell lines were a generous gift from Dr Ricardo Aguiar (University of Texas Health Science Center at San Antonio, San Antonio, TX, USA). PBMCs were purchased from PDXen Biosystems Co. Normal cells (splenocytes and bone marrow cells) from wild-type C57BL/6 mice were cultured in DMEM (Hyclone; Cytiva) with 10% FBS and 1% penicillin/streptomycin in a 5% CO₂ incubator at 37°C.

The primary antibodies against poly (ADP-ribose) polymerase 1 (PARP-1; cat. no. sc-7150, 1:1,000), pro-caspase 3 (cat. no. sc-7148, 1:1,000), Bcl-2 (cat. no. sc-7382, 1:2,000), Mcl-1 (cat. no. sc-819, 1:1,000), Bax (cat. no. sc-7480, 1:1,000), Bak (cat. no. sc-832, 1:1,000), Myc (cat. no. sc-40, 1:1,000), p53 (cat. no. sc-126, 1:1,000) and β -actin (cat. no. sc-47778, 1:1,000) were obtained from Santa Cruz Biotechnology, Inc. The antibody against Bcl-xL (cat. no. 14-6994-81, 1:1,000) was purchased from eBioscience. Secondary HRP-conjugated goat anti-rabbit (cat. no. A120-101p, 1:5,000) and secondary HRP-conjugated goat anti-mouse (cat. no. A90-116p, 1:5,000) IgG antibodies were obtained from Bethyl Laboratories.

Measurement of cell viability. The CellTiter 96 Aqueous MTS assay (Promega Corporation) was used to determine the cytotoxicity of DPSE or isolated compounds (1~6F and 1~6T), according to the manufacturer's instructions. Briefly, DLBCL and normal cells (splenocytes and bone marrow cells from mice and PBMCs) were plated at a density of 3x10⁴ cells and 5x10⁵ cells/well, respectively, in 96-well cell culture microplates and treated with DPSE (0, 0.2, 0.4, 0.6, 0.8 and 1 mg/ml for 24 or 48 h) or TLC fractions of terpenoids or flavonoids (0, 100 and 200 μ g/ml for 24 h) at 37°C, followed by the addition of 30 μ l MTS reagent to the wells and incubation at 37°C for 2 h. Absorbance was measured at 450 nm on a GloMax™ Microplate multi-mode reader (Promega Corporation).

Measurement of apoptotic rate, caspase-3/7 activities, and mitochondrial membrane potential. DHL4, Ly1, Ly8, HBL1 and normal murine cells were seeded at a density of 5x10⁵ cells/well in 12-well plates, treated with DPSE (0 and 1 mg/ml) for 24 h at 37°C, and stained using FITC

Annexin V Apoptosis Detection kit I (BD Biosciences) according to the manufacturer's instructions. The apoptotic fraction was analyzed by a BD FACSVerser flow cytometer (BD Biosciences). Data acquisition and analysis were performed using BD FACSCanto II software (version 3.0; BD Biosciences).

To examine caspase 3/7 activity, cells were exposed to DPSE (0, 0.5 and 1 mg/ml for 24 h) at 37°C, and Caspase-Glo 3/7 Assay reagent (cat. no. G8090; Promega Corporation) was added and incubated for 1 h at room temperature. Luminescence was measured using GloMax™ Microplate multi-mode reader.

For the measurement of the mitochondrial membrane potential, cells were treated with DPSE (0 or 1 mg/ml for 24 h) at 37°C, followed by the incubation with JC-1 dye (Abnova) for 15 min at 37°C. The resulting fluorescence was then monitored by fluorescence microscopy or by using a BD FACSVerser flow cytometer (BD Biosciences). Data acquisition and analysis were performed using DP2-BSW software (version 2.1; Olympus Cooperation) and BD FACSCanto II software (version 3.0; BD Biosciences).

Western blot analysis. Following exposure to DPSE (0, 0.5 or 1 mg/ml for 24 h at 37°C), DHL4, Ly1, Ly8, and HBL1 cells were harvested and lysed in RIPA buffer (ELPIS Biotech. Inc.) with 1 mM Na-vanadate, 50 mM β-glycerophosphate disodium salt, β-mercaptoethanol (142 mM; Bioworld Technology, Inc.), ProteaseArrest™ (G-Biosciences) and EDTA (5 mM; G-Biosciences). Protein concentrations were measured using the BCA assay kit (Thermo Fisher Scientific, Inc.) according to the manufacturer's instructions. Samples were boiled at 100°C for 10 min in sample buffer, 25 μg proteins were loaded in the 10 or 12% polyacrylamide gels, and transferred onto Immobilon-P Transfer membranes, followed by blocking with 1% bovine serum albumin (BSA; MP Biomedicals) for 1 h at room temperature and probing with primary antibodies at 4°C overnight. After washing three times with TBS containing 0.1% Tween-20 (TBST) for 5 min each, the membranes were probed with secondary anti-mouse/rabbit antibodies for 1 h at room temperature. After washing three times with TBST for 10 min each, the membranes were exposed to a chemiluminescent substrate [EzWestLumi plus (ATTO Corporation)] and the protein bands were visualized using the Luminograph II (ATTO Corporation). Western blots were quantified using ImageJ 1.52a software (National Institutes of Health).

Animal studies. For *in vitro* toxicity testing, the splenocytes and bone marrow cells were isolated from wild-type male C57BL/6 mice (n=5; age, 8 weeks; weight, 18±2 g), following the lysis of red blood cells using ammonium chloride-based red cell lysis buffer. For *in vivo* toxicity testing, 10 athymic male nude mice (age, 8 weeks; weight, 20±4 g) were divided into two groups and injected intraperitoneally with vehicle (1% methanol; n=5) or DPSE (50 mg/kg; n=5) daily for 3 weeks, followed by histological analysis of the lung, heart, liver and kidney. C57BL/6 and athymic nude mice (BALB/c-nu) were purchased from Central Lab Animal Inc. and Japan SLC, Inc., respectively. For xenograft studies, 6 athymic nude mice (age, 4 weeks; weight, 17±1.6 g) were divided into two cohorts and inoculated in the flanks with 1x10⁷ Ly1 or HBL1 parental cells. The injection sites were inspected for possible tumor formation for 3 weeks.

Mice were housed under a 12:12 h light/dark cycle at 26°C and provided food and water *ad libitum*. All mice used in this research were euthanized using a CO₂ chamber 3 weeks after the start of the indicated treatment. A 10-liter volume chamber was used and the displacement rate was fixed to 20% of the CO₂ chamber volume. Cervical dislocation was performed for secondary means to assure death after euthanasia. The animal protocol used in this study was reviewed and approved by the Pusan National University-Institutional Animal Care and Use Committee (approval no. PNU-2016-1158).

Hematoxylin and eosin (H&E) staining. H&E staining was performed as previously described (14,15). After sacrificing the mice, the lung, heart, liver and one kidney per mouse were isolated, and the specimens were fixed with 10% neutral buffered formalin solution (Sigma-Aldrich; Merck KGaA) at 4°C overnight. Then, samples were embedded in paraffin and cut into 4-μm sections, followed by deparaffinization, hydration and staining with H&E (stained with hematoxylin for 15 and eosin for 5 min) at room temperature. H&E-stained sections were visualized using a light microscope (Olympus CX31 microscope, Olympus Corporation) at x100 magnification. The representative images were captured using Motic Images Plus 2.0 software (Motic Co. Ltd.).

Ectopic expression of c-Myc in Ly1 cells. Generation of Ly1 control cells or Ly1 cells stably expressing c-Myc (Myc hereafter) using pCDH-CMV-MCS-EF1-copGFP lentiviral constructs (Systems Biosciences) was carried out as previously described (15), and then designated as Ly1 CDH and Ly1 CDH-Myc, respectively.

Reverse transcription-quantitative PCR (RT-qPCR). To measure the transcriptional level of Myc, total RNA was extracted from Ly1 CDH-control or CDH-Myc cells using TRIzol (Favorgen), and cDNA was synthesized using PrimeScript RT reagent kit with gDNA Eraser (Takara Bio, Inc.) according to the manufacturer's guidelines. qPCR was then performed using TOPreal qPCR PreMIX SYBR Green with low ROX (Enzynomics). The thermocycling conditions were as follows: 95°C for 10 min followed by 40 cycles of 95°C for 10 sec, 60°C for 15 sec and 72°C for 30 sec. The sequences for the TBP- and Myc-specific qPCR primers are as follows: Myc forward, 5'-CTCCTGGCAAAAGGTCAGAG-3' and reverse, 5'-TCGGTTGTTGCTGATCTGTC-3'; and TBP forward, 5'-TATAATCCCAAGCGGTTTGCTGCG-3' and reverse, 5'-AATTGTTGGTGGGTGAGACAAGG-3'. Relative gene expression was analyzed using the 2^{-ΔΔC_q} method (16).

Analysis of protein stability by the cycloheximide chase assay. To investigate Myc protein stability, Ly1 DLBCL cells were treated with cycloheximide (20 μg/ml; Sigma-Aldrich; Merck KGaA) in the presence or absence of DPSE (1 mg/ml for 0, 2, 4 or 8 h) (17). Western blotting was performed to analyze Myc protein levels.

Statistical analysis. Data are presented as the mean ± standard deviation. Statistically significant differences were identified by performing a Mann-Whitney U test or one-way ANOVA test with Tukey's post hoc test using Microsoft Office

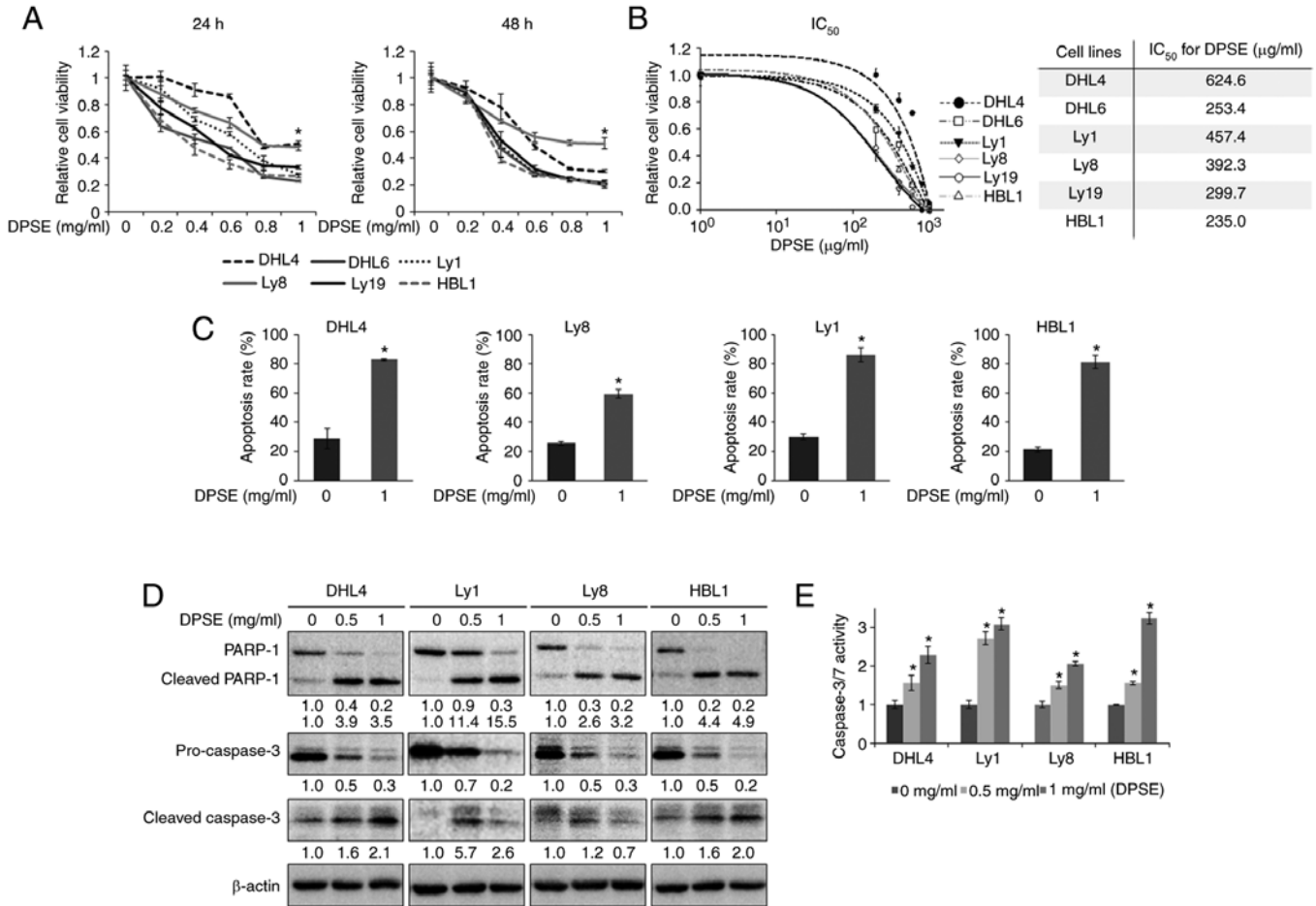


Figure 1. DPSE induces apoptosis in DLBCL cells by activating caspase-3/7. (A) Cell viability was measured by MTS assay after the exposure of multiple DLBCL cell lines to DPSE (0, 0.2, 0.4, 0.6, 0.8 and 1 mg/ml for 24 and 48 h). * $P < 0.05$ vs. 0 mg/ml DPSE. (B) The IC_{50} values for DPSE were calculated by using GraphPad Prism 5 software following treatment with increasing amounts of DPSE for 24 h. (C) The apoptotic rate was measured by flow cytometry after addition of DPSE (1 mg/ml for 24 h) in DHL4, Ly8, Ly1 and HBL1 cells. * $P < 0.05$ vs. 0 mg/ml DPSE. (D) Multiple DLBCL cell lines were treated with DPSE (0, 0.5 and 1 mg/ml for 24 h). Protein expression levels of PARP-1, cleaved PARP-1, pro-caspase 3, and cleaved caspase 3, which are markers for apoptosis, were assayed by western blotting in DHL4, Ly1, Ly8 and HBL1 cells. β -actin was used as a loading control. (E) Caspase-3/7 activities were analyzed using ELISA-based bioluminescence assays following treatment with DPSE (0, 0.5 and 1 mg/ml for 4, 8 or 12 h). * $P < 0.05$ vs. 0 mg/ml DPSE. DPSE, *Dracocephalum palmatum* Stephan extract; DLBCL, diffuse large B cell lymphoma; PARP-1, poly (ADP-ribose) polymerase 1.

Excel 2010 (Microsoft Corporation) and GraphPad Prism version5 software (GraphPad Software, Inc.). All experiments were repeated at least three times independently to confirm reproducibility. $P < 0.05$ was considered to indicate a statistically significant difference.

Results

DPSE induces apoptosis. To investigate the effect of DPSE on the survival of DLBCL cells, one ABC (HBL1) and five GCB DLBCL (DHL4, DHL6, Ly1, Ly8 and Ly19) cell lines were exposed to increasing concentrations of DPSE for 24 and 48 h, followed by MTS assay. Cell viability was decreased dose-dependently as compared with the control (Fig. 1A). The IC_{50} at 24 h ranged between 235.0 and 624.6 μ g/ml, and HBL1 and DHL4 cells were the most and least sensitive to DPSE, respectively (Fig. 1B). Annexin V/PI double staining demonstrated that the apoptotic rate was significantly increased upon exposure to DPSE (Figs. 1C and S1), which was associated with an increase in cleaved PARP-1, the active form of caspase 3, and caspase 3/7 activities (Fig. 1D and E).

To corroborate the *in vitro* results, *in vivo* studies were performed using murine xenograft models. Two cell lines, Ly1 and HBL1, were selected due to their robust proliferation in culture, and 1×10^7 Ly1 or HBL1 cells were injected subcutaneously into the flanks of athymic nude mice. However, tumors did not develop within 3 weeks (data not shown). Subsequently, the selectivity of DPSE toward cancer cells was investigated. Three different types of normal cells from humans and mice, human PBMCs, normal mouse splenocytes and bone marrow cells, were treated with DPSE, followed by the analysis of viability and apoptotic rates (Figs. 2A-C and S2). In contrast to DLBCL cells, the survival and apoptotic rates of normal cells were not affected, suggesting that the cytotoxic effect of DPSE is specific to cancer cells *in vitro*.

To further investigate the potential toxicity in normal cells, vehicle or DPSE was injected into athymic nude mice daily for 3 weeks. Tissues from the lung, heart, liver and kidney were then sectioned and H&E stained, followed by examination of their histopathology. Mice injected with either vehicle or DPSE did not show any obvious difference in terms of tissue architecture (Fig. 2D). Additionally, the measurement of body

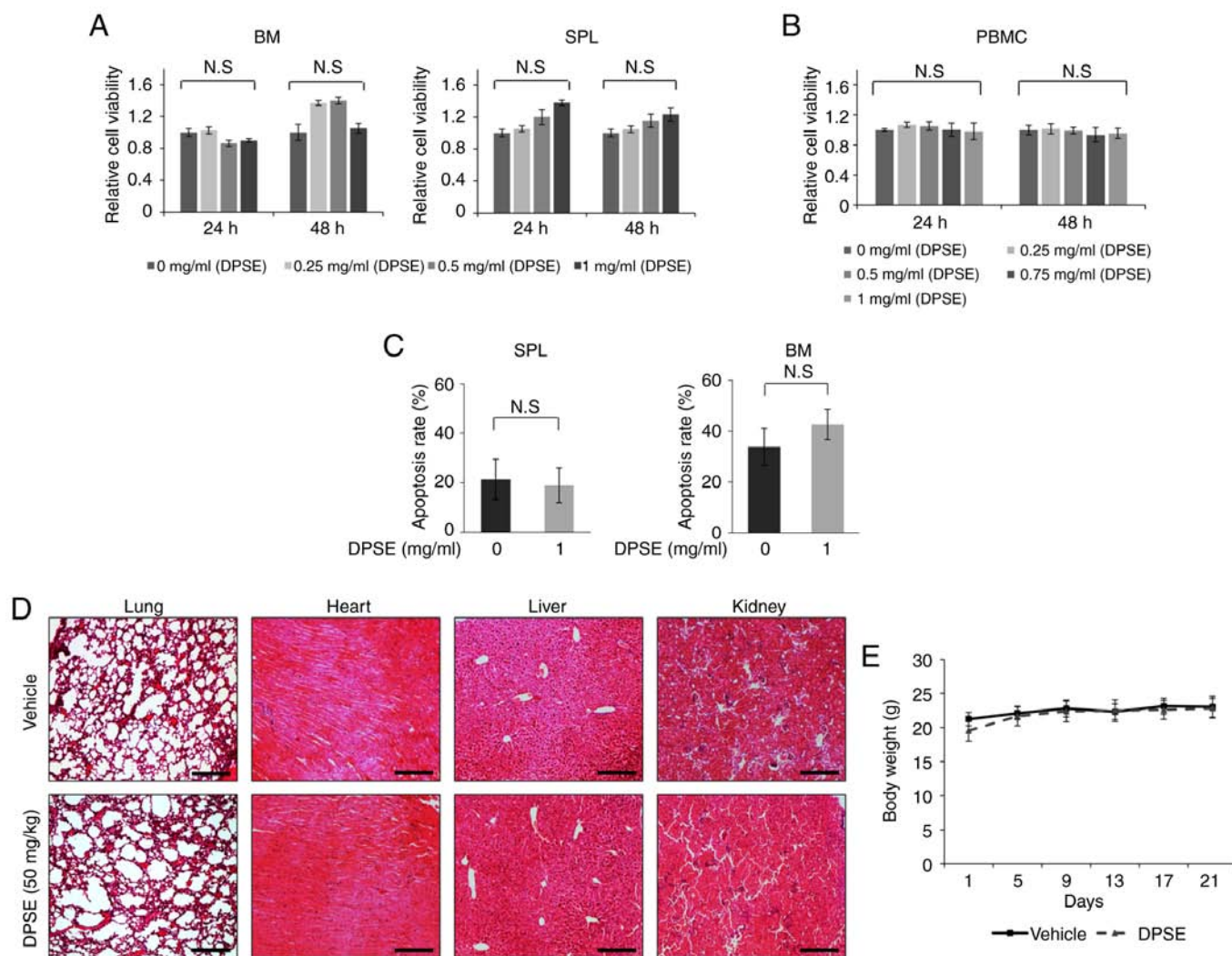


Figure 2. DPSE shows minimal toxicity toward normal cells *in vitro* and *in vivo*. (A) SPL and BM cells from wild-type C57BL/6 mice were exposed to DPSE (0, 0.25, 0.5 and 1 mg/ml) for 24 or 48 h, and MTS assays were conducted to measure cell viability. (B) Flow cytometry was used to identify apoptosis in normal mouse B cells after treatment with DPSE (0 and 1 mg/ml) for 24 h. (C) Human PBMCs were treated with DPSE (0, 0.25, 0.5, 0.75 and 1 mg/ml) for 24 or 48 h, and MTS assays were performed to analyze cell viability. (D) Athymic nude mice (BALB/c-nu, 4-weeks old, male) were treated with vehicle (1% methanol) or DPSE (50 mg/kg) daily for 3 weeks. Histological analysis of the lung, heart, liver and kidney sections after exposure to DPSE were carried out by hematoxylin and eosin staining Magnification, x100. Scale bar, 100 μ m. (E) Mouse body weights were measured every 4 days during the administration of DPSE. N.S., not significant; SPL, splenocyte; BM, bone marrow; PBMC, peripheral blood mononuclear cell; DPSE, *Dracocephalum palmatum* Stephan extract.

weights during drug administration suggests no systemic toxicity from DPSE treatment (Fig. 2E). These results collectively demonstrate that DPSE has minimal toxicity in normal cells and specifically affects cancer cells.

Apoptosis induced by DPSE relies on caspases and mitochondria. The increase in the cleaved/active form of caspase-3 and caspase-3/7 activities (Fig. 1D and E) indicates the involvement of these proteins in DPSE-induced cell killing. Therefore, the present study investigated the mechanism by which DPSE activates caspase-3/7 in DLBCL. It is well-established that an unbalanced ratio between pro- and anti-apoptotic Bcl-2 family members triggers disruption of mitochondrial membrane potential, which leads to cytochrome *c* release into the cytoplasm that culminates in the activation of caspases (18). Administration of DPSE markedly suppressed the levels of pro-survival proteins Mcl-1 and Bcl-xL (Fig. 3A), while it augmented the expression of pro-apoptotic

Bax and Bak (Fig. 3B). This effect of DPSE was tightly associated with decreased mitochondrial membrane potential, which was confirmed by fluorescence microscopy and flow cytometry (Fig. 3C-E). Together, these data suggest that DPSE induces apoptosis in DLBCL by disrupting the mitochondrial membrane potential and increasing activities of caspases.

Myc appears to be an important regulator of DPSE-induced cell death. We and others have previously shown that apoptosis of DLBCL cells could be induced when Myc is downregulated by Myc inhibitors JQ1 and 10058-F4 (14,19). To investigate the potential involvement of Myc in DPSE-induced apoptosis, four different DLBCL cell lines were treated with DPSE for 24 h and it was identified that Myc levels were markedly reduced (Fig. 4A). Next, the present study aimed to determine whether DPSE affects Myc expression at the transcriptional or post-transcriptional level. The mRNA level of Myc was significantly downregulated upon treatment with DPSE (Fig. 5A),

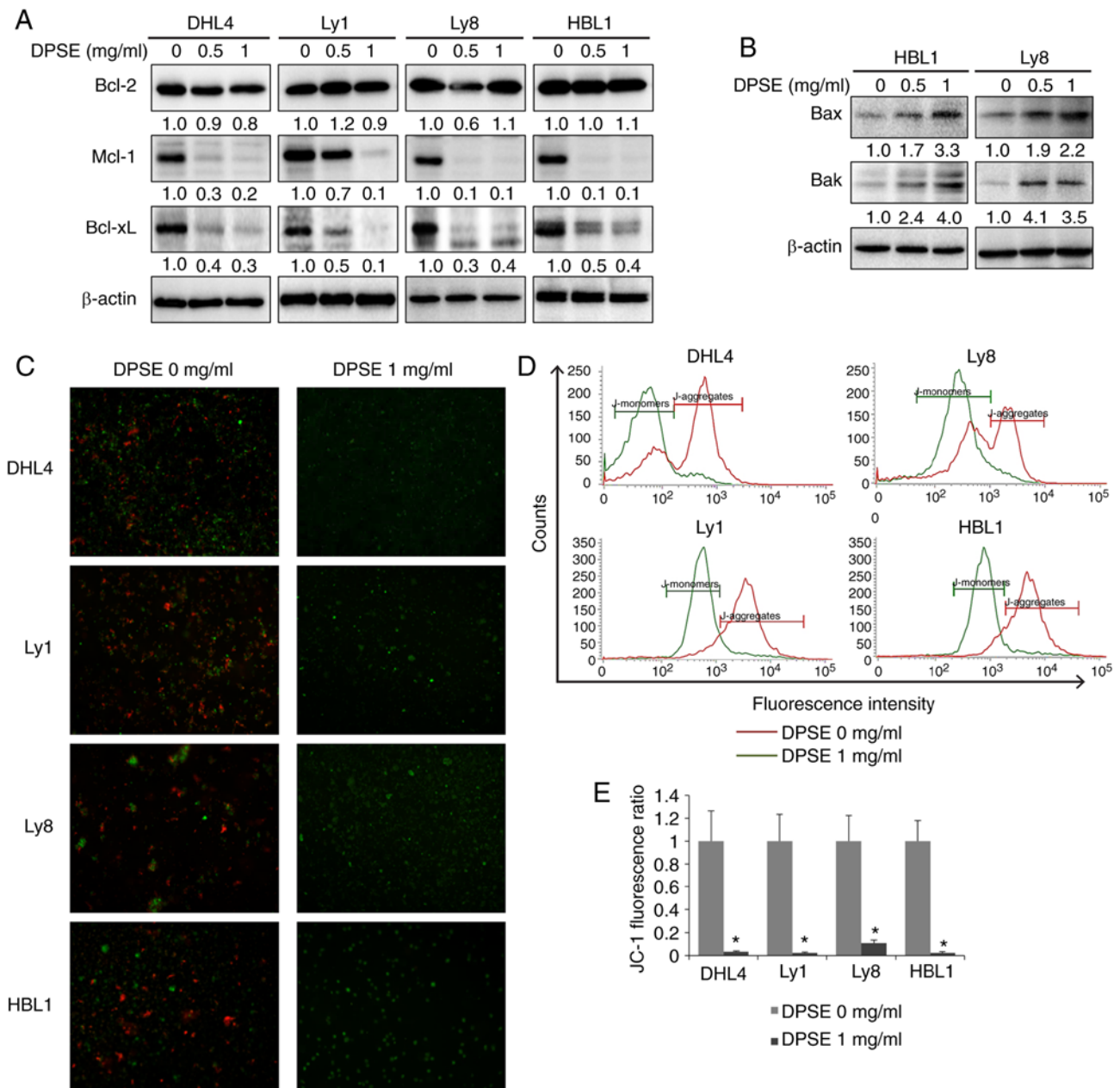


Figure 3. DPSE modulates the levels of pro- and anti-apoptotic Bcl-2 family members, and decreases mitochondrial potential. (A) DHL4, Ly1, Ly8 and HBL1 cells were exposed to DPSE (0, 0.5 and 1 mg/ml) for 24 h, and protein expression levels of anti-apoptotic Bcl-2 family members Bcl-2, Mcl-1 and Bcl-xL were assayed by western blotting. (B) Ly1 and HBL1 cells were treated with DPSE (0, 0.5 and 1 mg/ml) for 1 h, and the expression of pro-apoptotic Bcl-2 family members Bax and Bak was assayed by western blotting. DHL4, Ly1, Ly8 and HBL1 cells were stained with JC-1 following the addition of vehicle or DPSE (1 mg/ml for 24 h), and staining was monitored by (C) fluorescence microscopy or (D) flow cytometry. (E) Mitochondrial membrane potential was determined by calculating the JC-1 fluorescence ratio of J-aggregates (red) to J-monomers (green). * $P < 0.05$ vs. 0 mg/ml DPSE. DPSE, *Dracocephalum palmatum* Stephan extract.

and Myc protein was less stable in the presence of DPSE when protein biosynthesis was inhibited by cycloheximide (Fig. 5B). These data clearly demonstrated that DPSE modulates Myc levels both transcriptionally and post-transcriptionally. To directly test whether Myc plays a critical role in DPSE-induced apoptosis, Ly1 cells ectopically expressing Myc were generated (Fig. S3). Ly1 parental cells and Ly1 cells transduced with a control vector exhibited a similar sensitivity to DPSE, while Ly1 cells transduced with a vector expressing Myc were significantly more resistant to DPSE treatment (Fig. 4B). Furthermore, Myc expression was inhibited by DPSE in Ly1

parental and Ly1 CDH control cells, but not in Ly1 CDH-Myc overexpressing cells (Fig. 4C). The same phenomenon was observed with JQ1, a well-characterized Myc inhibitor (20). In this previous study, JQ1 suppressed endogenous, but not exogenous, Myc expression, and ectopic Myc expression using the MSCV retroviral vector abolished the negative impact of JQ1 on cell proliferation. When treated with JQ1, the fractions of control and Myc-overexpressing cells in the S phase was decreased by 51 and 24%, respectively (20). Taken together, the results indicate that DPSE-triggered cell death is accomplished via, at least in part, a downregulation of Myc.

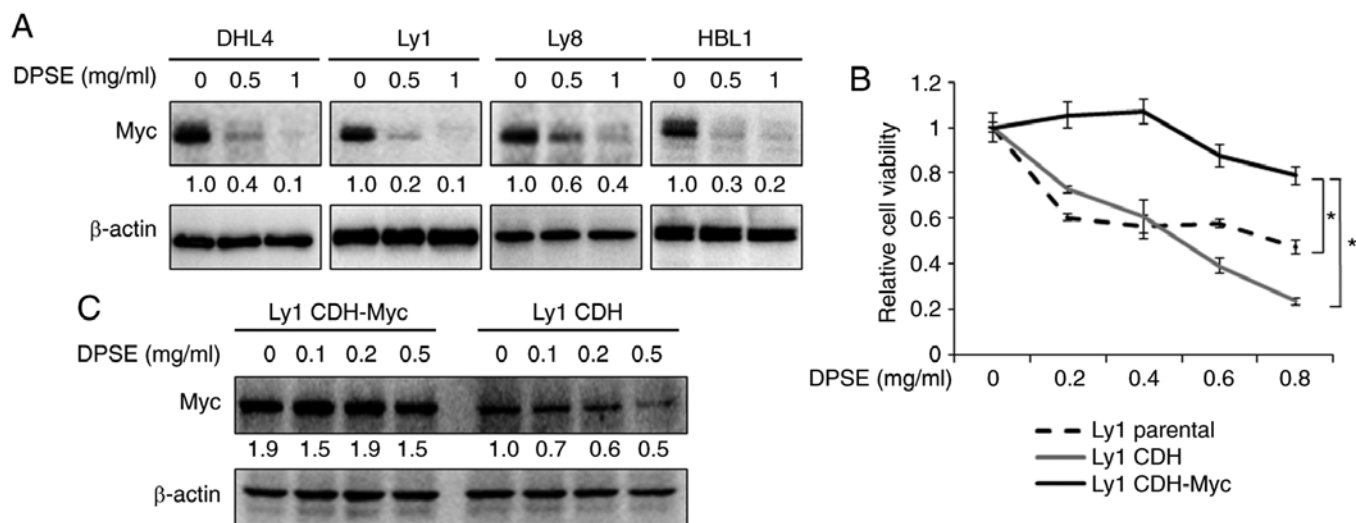


Figure 4. DPSE-induced cell death may be mediated by Myc. (A) DHL4, Ly1, Ly8, and HBL1 cells were exposed to DPSE (0, 0.5 and 1 mg/ml) for 24 h and protein expression levels of Myc were analyzed by western blotting. (B) Ly1 parental, CDH-control or CDH-Myc cells were treated with DPSE (0, 0.2, 0.4, 0.6 and 0.8 mg/ml for 24 h), and cell viability was measured by MTS assay. (C) Ly1 CDH-control or CDH-Myc cells were exposed to DPSE (0, 0.1, 0.2 and 0.5 mg/ml) for 12 h, and protein levels of Myc were examined by western blotting. * $P < 0.05$. DPSE, *Dracocephalum palmatum* Stephan extract; CDH, vector.

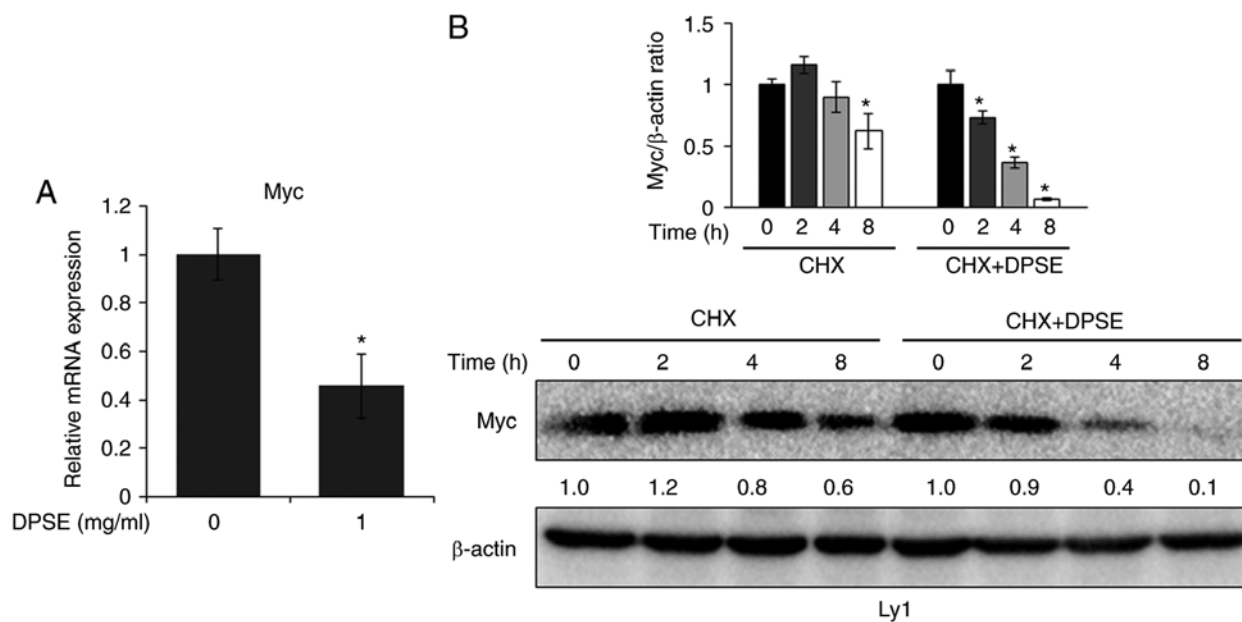


Figure 5. DPSE modulates Myc expression at the transcriptional and post-transcriptional level. (A) Myc mRNA levels were measured by reverse transcription-quantitative PCR after treatment with DPSE (0 and 1 mg/ml for 24 h). (B) Ly1 cells were exposed to either vehicle or DPSE (0 and 1 mg/ml for 0, 2, 4, and 8 h) in the presence of CHX (20 μ g/ml); then, protein stability was analyzed by western blotting. * $P < 0.05$ vs. 0 mg/ml DPSE. DPSE, *Dracocephalum palmatum* Stephan extract; CHX, cycloheximide.

TLC fractionation of DPSE and LC/MS profile of the fraction with apoptotic effect. A previous study have shown that terpenoid and flavonoid compounds have anticancer activities (21). To gain insight into the nature of apoptosis-inducing compounds in DPSE, TLC fractionation was performed that resulted in total 12 fractions of terpenoids (1T-6T) and flavonoids (1F-6F). Ly1 and DHL4 DLBCL cells were exposed to each fraction for 24 h and cell viability was examined by the MTS assays. None of the terpenoid fractions elicited any discernible cytotoxic effect (Fig. S4). A significant dose-dependent decrease in cell viability was observed only with 6F, implying that most, if not

all, of anti-lymphoma effect of DPSE stems from flavonoid compounds in 6F (Figs. 6A and S5).

The present study performed Annexin V/PI staining followed by FACS analysis to examine the apoptotic fraction after 6F treatment. Consistently, the apoptotic rate was significantly increased when Ly1 cells were exposed to 6F for 24 h (Figs. 6B and S6). To gain mechanistic insight into 6F-induced apoptosis, the levels of Myc and anti- and pro-apoptotic Bcl2 family proteins were examined after treatment with 6F. Myc and anti-apoptotic Bcl2 members, Mcl-1 and Bcl-xL, were significantly downregulated, while pro-apoptotic proteins

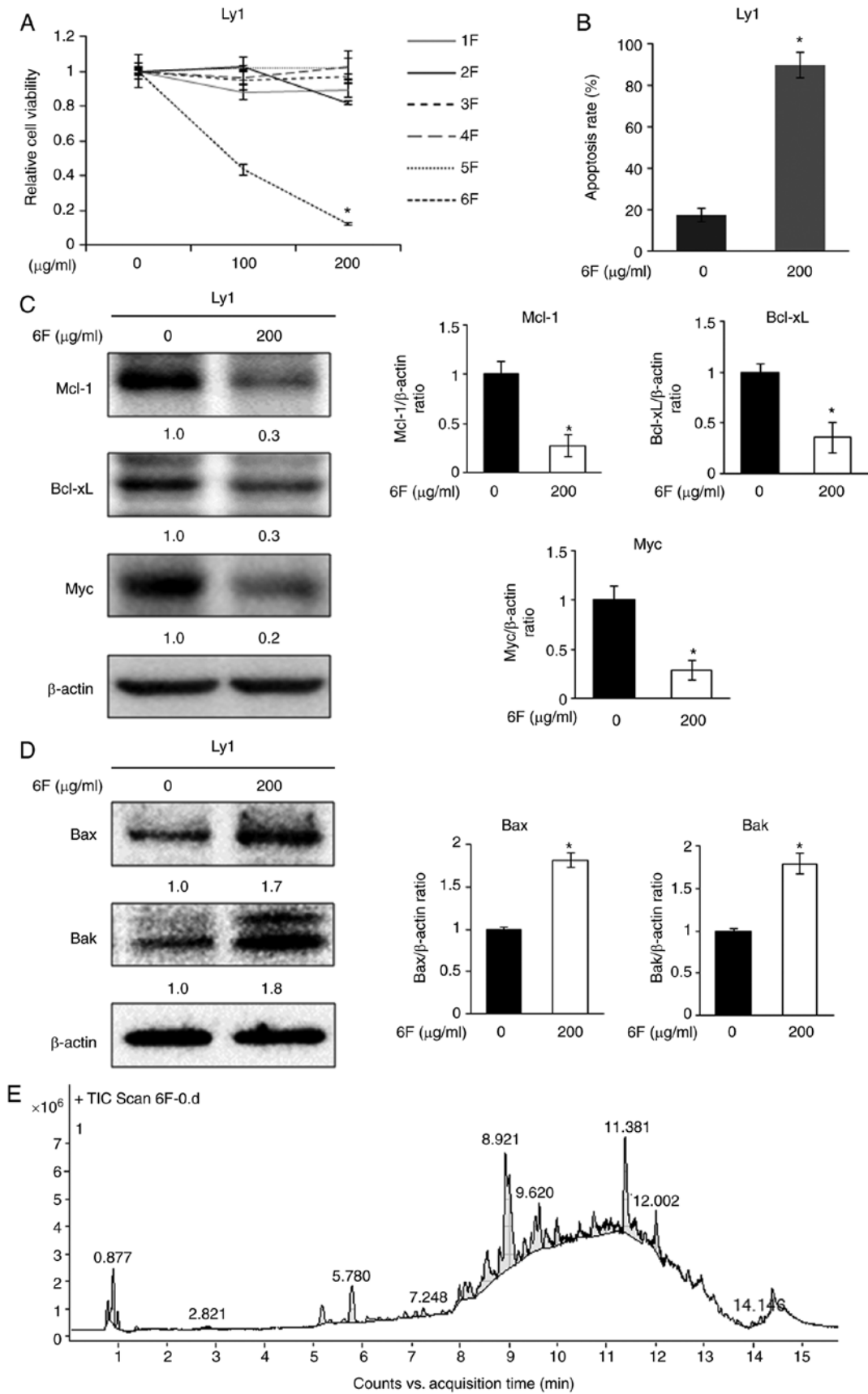


Figure 6. Cytotoxic effects of the TLC fractions of DPSE on diffuse large B cell lymphoma cells. (A) Ly1 and DHL4 cells were exposed to the fractions 1F-6F of DPSE (0, 100 and 200 µg/ml for 24 h), followed by the measurement of cell viability. *P<0.05 vs. 0 µg/ml 1F-6F. (B) Ly1 cells were treated with 6F of DPSE (0 and 200 µg/ml for 24 h), and the apoptotic rate was measured by Annexin V/PI staining and FACS analysis. *P<0.05 vs. 0 mg/ml DPSE. (C) The levels of Myc and anti-apoptotic Bcl2 family members, Mcl-1 and Bcl-xL, were examined by western blotting after treatment with 6F (0 and 200 µg/ml for 24 h). *P<0.05 vs. 0 mg/ml DPSE. (D) The expression of pro-apoptotic Bcl2 members Bak and Bax was analyzed by western blotting upon exposure to 6F (0 and 200 µg/ml for 24 h). *P<0.05 vs. 0 mg/ml DPSE. (E) Liquid chromatography/mass spectrometry profile of the TLC fraction 6F of DPSE. TLC, thin layer chromatography; DPSE, *Dracocephalum palmatum* Stephan extract.

Table I. Molecular formulas and m/z values for the main compounds in the fraction 6F of *Dracocephalum palmatum* Stephan extract by liquid chromatography/mass spectrometry in the positive ionization mode.

Retention time, min	m/z	Adduct ions	Molecular formula
0.877	479.032	(M+H) ⁺	C ₁₆ H ₁₄ O ₁₇
5.170	393.144	(M+Na) ⁺	C ₂₅ H ₂₂ O ₃
5.780	435.082	(M+Na) ⁺	C ₂₅ H ₁₆ O ₆
7.660	599.390	(M+H) ⁺	C ₃₆ H ₅₄ O ₇
8.556	207.099	(M+Na) ⁺	C ₁₀ H ₁₆ O ₃
8.921	557.276	(M+H) ⁺	C ₃₁ H ₄₀ O ₉
9.398	611.271	(M+H) ⁺	C ₃₀ H ₄₂ O ₁₃
9.974	819.372	(M+Na) ⁺	C ₄₇ H ₅₆ O ₁₁
11.381	773.493	(M+H) ⁺	C ₅₅ H ₆₄ O ₃
12.002	455.350	(M+Na) ⁺	C ₂₈ H ₄₆ O ₃

Bax and Bak were significantly upregulated (Fig. 6C and D). These data suggest that 6F-induced apoptosis is tightly associated with down- and upregulation of anti- and pro-apoptotic factors, respectively. Next, HPLC/MS analysis was conducted to identify molecular formulas of flavonoids in 6F, and the most abundant compounds separated by the LC peaks are integrated (Fig. 6E and Table I). Expanded analyses of these integrated peaks from MS data are presented in Table SI.

Taken together, the data revealed the anticancer effect of DPSE in DLBCL and the underlying mechanism. DPSE-induced cell killing was shown to be mediated by disruption of the mitochondrial membrane potential via an imbalance between pro- and anti-apoptotic Bcl-2 proteins, in which p53 and Myc play a central role as upstream regulators of Bcl-2 family proteins (Fig. 7 and S7).

Discussion

Palmate dragonhead DPS has been traditionally used for the treatment of gastrointestinal tract disorders and as a diuretic and a choleric remedy by the North-Yakutian nomads in Russia (12). A previous study has shown that DPSE has a strong antioxidant effect (12). The present study tested a potential use of this plant extract as an anticancer agent and elucidated the underlying mechanism. It was identified that the plant extract efficiently induced apoptosis in multiple DLBCL cell lines with minimal toxicity in normal cells *in vitro* and *in vivo*. This effect involved the depolarization of the mitochondrial membrane potential and subsequent caspase activation. Additionally, the current study revealed the involvement of Myc in DPSE-induced cell death. It is not clear whether DPSE would have any effect on the GCB- and ABC-DLBCL primary cells. Based on the present *in vitro* results using GCB (DHL4, DHL6, Ly1, Ly8, and Ly19) and ABC (HBL1) DLBCL cell lines, it was predicted that DPSE can kill both GCB- and ABC-DLBCL primary cells. We as well as other researchers have demonstrated that Myc is frequently dysregulated in both subtypes of DLBCL and plays a critical role in their survival (14,19); moreover, the present study has indicated that DPSE-induced death of DLBCL cells depends on Myc inhibition. It can therefore be hypothesized

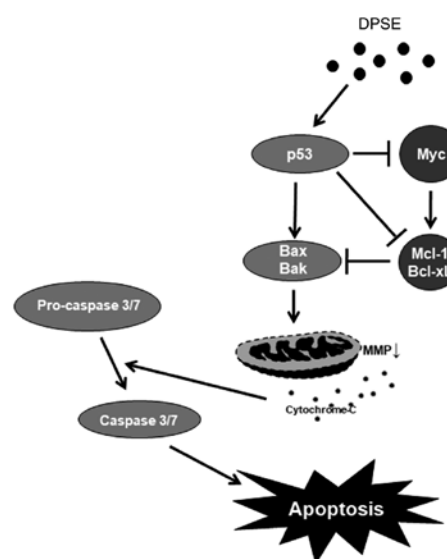


Figure 7. Schematic of DPSE-induced cell death. DPSE-induced cell death may involve upregulation of the p53 tumor suppressor and downregulation of the Myc oncoprotein, which modulates the expression of pro- and anti-apoptotic Bcl-2 proteins, thus tipping the balance towards apoptosis. Disruption of the balance between pro- and anti-apoptotic Bcl-2 family members is known to decrease the mitochondrial membrane potential, subsequently leading to the release of cytochrome c, activation of caspase 3/7, and eventually cell death. The expression of pro-survival Bcl-2 family members Mcl-1 and Bcl-xL may become abnormally high due to the dysregulation of Myc, which may overwhelm the tumor-suppressive function of p53, and consequently, abolish DPSE-induced apoptosis. MMP, mitochondrial membrane potential; DPSE, *Dracocephalum palmatum* Stephan extract.

that one of the primary targets of DPSE is Myc and this would be clarified upon isolating and characterizing the compounds in DPSE with pro-apoptotic activities. The present work lacks *in vivo* studies and human primary DLBCL data, which could be a limitation of the study.

It has previously been shown that Myc is frequently dysregulated by various mechanisms in different types of human cancers, such as t(8;14)(q24;q32) translocation involving IgH and Myc in B-cell lymphomas, and APC inactivation and subsequent hyperactivation of Wnt/Myc axis in colon cancers (22-25). Myc plays a critical role in the survival of

cancer cells and administration of Myc inhibitors alone or in combination with other anticancer agents elicits cytotoxicity in these cancer cells (14,26,27). The present results that demonstrated downregulation of Myc was associated with death of DLBCL cells upon exposure to DPSE clearly indicates the potential use of DPSE for the treatment of patients with this disease with minimum side effects. Given that the DLBCL cell lines that were used in the current study exhibit different Myc status (Myc is amplified in DHL4 and translocated in Ly1, Ly8 and HBL1) (19,26), DPSE can be used to downregulate Myc regardless of the Myc status. The present data show that Myc expression can be regulated by DPSE both transcriptionally and post-transcriptionally.

Primary targets of DPSE are yet to be identified. However, based on the current data that DPSE exerts a pro-apoptotic effect in a Myc-dependent manner, it can be proposed that the primary targets of DPSE may be direct or indirect regulators of Myc. One of the well-characterized transcriptional repressors of Myc is the p53 tumor suppressor (28). The present data demonstrated that DPSE significantly increases p53 expression, which is associated with Myc suppression. However, the possibility that Myc expression is regulated by DPSE through other ways cannot be excluded, which would be clarified upon isolating the pro-apoptotic components of DPSE.

Notably, the levels of pro-survival Bcl-2 protein were unchanged upon addition of the extract, suggesting that other Bcl-2 family members, such as Mcl-1 and Bcl-xL, may be major players in DPSE-triggered apoptosis. Mcl-1 has been shown to be commonly upregulated in cancer and its high levels confers resistance to ABT-737, a Bcl-2 small molecule inhibitor as a BH3 mimetic (29,30). The present results that DPSE efficiently downregulates Mcl-1 provides a rational for combining DPSE with the Bcl-2 inhibitor ABT-737 to overcome the chemoresistance.

The present study characterized the molecular formulas of the major flavonoid compounds with anti-lymphoma effects in a fraction after partial purification of DPSE by TLC fractionation. There are several predicted compounds in 6F, such as benzoic acid and gustastatin, with a potential anti-lymphoma activity. Benzoic acid and its derivatives are found in a number of plants, including cinnamon, cloves, tomatoes and berries, and are known to inhibit cell growth by ameliorating angiogenesis and invasion in cervical cancer cells (31). Gustastatin was originally isolated from the Brazilian nut tree *Gustavia hexapetala* (32) and was found in *Cupania cinerea* (33). This compound with anticancer activities can be chemically synthesized and is commercially available (34). New compounds with antitumor activities can possibly be isolated, but further research is required to elucidate the exact components in 6F and their structures.

In conclusion, the present study revealed a previously uncharacterized anticancer effect of DPSE and the mechanism by which DPSE induces apoptosis in DLBCL cells. Previous observations (35-38) and our current work suggest that a major target of DPSE may be the p53 tumor suppressor that can modulate the expression of Bcl-2 family members directly or indirectly via Myc inhibition, leading to the disruption of mitochondrial membrane potential, caspase activation and apoptosis (Fig. 7). Notably, ectopic expression of Myc rescues DPSE-triggered cell death. Although further mechanistic insights into the anticancer

activities of DPSE are required, the present results suggests that inhibition of Myc may enhance the pro-apoptotic effect of DPSE, and co-treatment of DPSE and Myc inhibitors such as JQ1 may induce synergistic killing of tumor cells, which could provide a novel therapeutic strategy for patients with DLBCL.

Acknowledgements

The DHL4, DHL6, Ly1, Ly8, Ly19 and HBL1 DLBCL cell lines were a generous gift from Dr Ricardo Aguiar (University of Texas Health Science Center at San Antonio, San Antonio, TX, USA).

Funding

This work was supported by the Basic Science Research Program through the National Research Foundation of Korea funded by the Ministry of Science, ICT & Future Planning (grant no. 2019R1F1A1060565).

Availability of data and materials

The datasets used and/or analyzed during the current study are available from the corresponding author on reasonable request.

Authors' contributions

JK performed the experiments, analyzed the data and wrote the paper. JNK, IP and SS performed the experiments and analyzed the data. ZO and ISZ contributed to the conception of the study, supervised the study and wrote the manuscript. SWK designed and supervised the study, contributed to the conception of the study, planned the experiments, analyzed the data and wrote the paper. All authors read and approved the final manuscript.

Ethics approval and consent to participate

The animal protocol used in this study was reviewed and approved by the Pusan National University-Institutional Animal Care and Use Committee (approval no PNU-2016-1158).

Patient consent for publication

Not applicable.

Competing interests

The authors declare that they have no competing interests.

References

1. Lenz G and Staudt LM: Aggressive lymphomas. *N Engl J Med* 362: 1417-1419, 2010.
2. Alizadeh AA, Eisen MB, Davis RE, Ma C, Lossos IS, Rosenwald A, Boldrick JC, Sabet H, Tran T, Yu X, *et al*: Distinct types of diffuse large B-cell lymphoma identified by gene expression profiling. *Nature* 403: 503-511, 2000.
3. Compagno M, Lim WK, Grunn A, Nandula SV, Brahmachary M, Shen Q, Bertoni F, Ponzoni M, Scandurra M, Califano A, *et al*: Mutations of multiple genes cause deregulation of NF-kappaB in diffuse large B-cell lymphoma. *Nature* 459: 717-721, 2009.

4. Coiffier B, Lepage E, Briere J, Herbrecht R, Tilly H, Bouabdallah R, Morel P, Van Den Neste E, Salles G, Gaulard P, *et al*: CHOP chemotherapy plus rituximab compared with CHOP alone in elderly patients with diffuse large-B-cell lymphoma. *N Engl J Med* 346: 235-242, 2002.
5. Coiffier B: Rituximab therapy in malignant lymphoma. *Oncogene* 26: 3603-3613, 2007.
6. Pasqualucci L and Dalla-Favera R: The genetic landscape of diffuse large B-cell lymphoma. *Semin Hematol* 52: 67-76, 2015.
7. Hengartner MO: The biochemistry of apoptosis. *Nature* 407: 770-776, 2000.
8. Cleveland JL and Ihle JN: Contenders in FasL/TNF death signaling. *Cell* 81: 479-482, 1995.
9. Elmore S: Apoptosis: A review of programmed cell death. *Toxicol Pathol* 35: 495-516, 2007.
10. Green DR: The coming decade of cell death research: Five riddles. *Cell* 177: 1094-1107, 2019.
11. Green DR and Reed JC: Mitochondria and apoptosis. *Science* 281: 1309-1312, 1998.
12. Olennikov DN, Chirikova NK, Okhlopkova ZM and Zulfugarov IS: Chemical composition and antioxidant activity of Tánara Ótó (*Dracocephalum palmatum* Stephan), a medicinal plant used by the North-Yakutian nomads. *Molecules* 18: 14105-14121, 2013.
13. Jeong D, Kim J, Nam J, Sun H, Lee YH, Lee TJ, Aguiar RC and Kim SW: MicroRNA-124 links p53 to the NF- κ B pathway in B-cell lymphomas. *Leukemia* 29: 1868-1874, 2015.
14. Kim E, Nam J, Chang W, Zulfugarov IS, Okhlopkova ZM, Olennikov D, Chirikova NK and Kim SW: *Angelica gigas* Nakai and decursin downregulate Myc expression to promote cell death in B-cell lymphoma. *Sci Rep* 8: 10590, 2018.
15. Nam J, Kim DU, Kim E, Kwak B, Ko MJ, Oh AY, Park BJ, Kim YW, Kim A, Sun H, *et al*: Disruption of the Myc-PDE4B regulatory circuitry impairs B-cell lymphoma survival. *Leukemia* 33: 2912-2923, 2019.
16. Livak KJ and Schmittgen TD: Analysis of relative gene expression data using real-time quantitative PCR and the 2(-Delta Delta C(T)) method. *Methods* 25: 402-408, 2001.
17. Kao SH, Wang WL, Chen CY, Chang YL, Wu YY, Wang YT, Wang SP, Nesvizhskii AI, Chen YJ, Hong TM and Yang PC: Analysis of protein stability by the cycloheximide chase assay. *Bio Protoc* 5: e1374, 2015.
18. Chipuk JE and Green DR: How do BCL-2 proteins induce mitochondrial outer membrane permeabilization? *Trends Cell Biol* 18: 157-164, 2008.
19. Trabucco SE, Gerstein RM, Evens AM, Bradner JE, Shultz LD, Greiner DL and Zhang H: Inhibition of bromodomain proteins for the treatment of human diffuse large B-cell lymphoma. *Clin Cancer Res* 21: 113-122, 2015.
20. Delmore JE, Issa GC, Lemieux ME, Rahl PB, Shi J, Jacobs HM, Kastriitis E, Gilpatrick T, Paranal RM, Qi J, *et al*: BET bromodomain inhibition as a therapeutic strategy to target c-Myc. *Cell* 146: 904-917, 2011.
21. Zheng GQ: Cytotoxic terpenoids and flavonoids from *Artemisia annua*. *Planta Med* 60: 54-57, 1994.
22. Ott G, Rosenwald A and Campo E: Understanding MYC-driven aggressive B-cell lymphomas: Pathogenesis and classification. *Blood* 122: 3884-3891, 2013.
23. Sansom OJ, Meniel VS, Muncan V, Pheesse TJ, Wilkins JA, Reed KR, Vass JK, Athineos D, Clevers H and Clarke AR: Myc deletion rescues Apc deficiency in the small intestine. *Nature* 446: 676-679, 2007.
24. Kwak B, Kim DU, Kim TO, Kim HS and Kim SW: MicroRNA-552 links Wnt signaling to p53 tumor suppressor in colorectal cancer. *Int J Oncol* 53: 1800-1808, 2018.
25. Sewastianik T, Prochorec-Sobieszek M, Chapuy B and Juszczynski P: MYC deregulation in lymphoid tumors: Molecular mechanisms, clinical consequences and therapeutic implications. *Biochim Biophys Acta* 1846: 457-467, 2014.
26. Li W, Gupta SK, Han W, Kundson RA, Nelson S, Knutson D, Greipp PT, Elsayfa SF, Sotomayor EM and Gupta M: Targeting MYC activity in double-hit lymphoma with MYC and BCL2 and/or BCL6 rearrangements with epigenetic bromodomain inhibitors. *J Hematol Oncol* 12: 73, 2019.
27. Tan Z, Zhang X, Kang T, Zhang L and Chen S: Arsenic sulfide amplifies JQ1 toxicity via mitochondrial pathway in gastric and colon cancer cells. *Drug Des Devel Ther* 12: 3913-3927, 2008.
28. Ho JS, Ma W, Mao DY and Benchimol S: p53-Dependent transcriptional repression of c-myc is required for G1 cell cycle arrest. *Mol Cell Biol* 25: 7423-7431, 2005.
29. Oltersdorf T, Elmore SW, Shoemaker AR, Armstrong RC, Augeri DJ, Belli BA, Bruncko M, Deckwerth TL, Dinges J, Hajduk PJ, *et al*: An inhibitor of Bcl-2 family proteins induces regression of solid tumours. *Nature* 435: 677-681, 2005.
30. van Delft MF, Wei AH, Mason KD, Vandenberg CJ, Chen L, Czabotar PE, Willis SN, Scott CL, Day CL, Cory S, *et al*: The BH3 mimetic ABT-737 targets selective Bcl-2 proteins and efficiently induces apoptosis via Bak/Bax if Mcl-1 is neutralized. *Cancer Cell* 10: 389-399, 2006.
31. Zhao B and Hu M: Gallic acid reduces cell viability, proliferation, invasion and angiogenesis in human cervical cancer cells. *Oncol Lett* 6: 1749-1755, 2013.
32. Pettit GR, Zhang Q, Pinilla V, Herald DL, Doubek DL and Duke JA: Isolation and structure of gustastatin from the Brazilian nut tree *Gustavia hexapetalata*. *J Nat Prod* 67: 983-985, 2004.
33. Malagón O, Ramirez J, Andrade JM, Morocho V, Armijos C and Gilardoni G: Phytochemistry and ethnopharmacology of the Ecuadorian flora. A review. *Nat Prod Commun* 11: 297-314, 2016.
34. García-Fortanet J, Debergh JR and De Brabander JK: A photochemical entry to depsides: Synthesis of gustastatin. *Org Lett* 7: 685-688, 2005.
35. Kroemer G, Galluzzi L and Brenner C: Mitochondrial membrane permeabilization in cell death. *Physiol Rev* 87: 99-163, 2007.
36. Kuwana T, Mackey MR, Perkins G, Ellisman MH, Latterich M, Schneider R, Green DR and Newmeyer DD: Bid, Bax, and lipids cooperate to form supramolecular openings in the outer mitochondrial membrane. *Cell* 111: 331-342, 2002.
37. Labisso WL, Wirth M, Stojanovic N, Stauber RH, Schnieke A, Schmid RM, Krämer OH, Saur D and Schneider G: MYC directs transcription of MCL1 and eIF4E genes to control sensitivity of gastric cancer cells toward HDAC inhibitors. *Cell Cycle* 11: 1593-1602, 2012.
38. Wei MC, Zong WX, Cheng EH, Lindsten T, Panoutsakopoulou V, Ross AJ, Roth KA, MacGregor GR, Thompson CB and Korsmeyer SJ: Proapoptotic BAX and BAK: A requisite gateway to mitochondrial dysfunction and death. *Science* 292: 727-730, 2001.